the FEBS Journal

Characterization of inhibitory mechanism and antifungal activity between group-1 and group-2 phytocystatins from taro (*Colocasia esculenta*)

Ke-Ming Wang[1], Senthil Kumar[1], Yi-Sheng Cheng[1,2], Shripathi Venkatagiri[3], Ai-Hwa Yang[4] and Kai-Wun Yeh[1]

1 Institute of Plant Biology, National Taiwan University, Taipei, Taiwan
2 Department of Life Science, National Taiwan University, Taipei, Taiwan
3 Department of Botany, Karnatak University, Dharwad, India
4 Tainan District of Agricultural Improvement and Extension Station, Council of Agriculture, Tainan, Taiwan

Keywords
allosteric activation; anti-fungal activity; cysteine proteinase inhibitor; inhibitory kinetics; tarocystatin (CeCPI)

Correspondence
K.-W. Yeh, Institute of Plant Biology, National Taiwan University, Taipei 106, Taiwan
Fax: +886 2 23622703
Tel: +886 2 33662536
E-mail: ykwbppp@ntu.edu.tw

(Received 10 June 2008, revised 5 August 2008, accepted 7 August 2008)

doi:10.1111/j.1742-4658.2008.06631.x

Tarocystatin from *Colocasia esculenta*, a group-2 phytocystatin, is a defense protein against phytopathogenic nematodes and fungi. It is composed of a highly conserved N-terminal region, which is homological to group-1 cystatin, and a repetitive peptide at the C-terminus. The purified recombinant proteins of tarocystatin, such as full-length (FL), N-terminus (Nt) and C-terminus (Ct) peptides, were produced and their inhibitory activities against papain as well as their antifungal effects were investigated. Kinetic analysis revealed that FL peptide exhibited mixed type inhibition (K_{ia} = 0.098 μM and K_{ib} = 0.252 μM) and Nt peptide showed competitive inhibition (K_i = 0.057 μM), whereas Ct peptide possessed weak papain activation properties. A shift in the inhibitory pattern from competitive inhibition of Nt peptide alone to mixed type inhibition of FL peptide implied that the Ct peptide has an regulatory effect on the function of FL peptide. Based on the inhibitory kinetics of FL (group-2) and Nt (group-1) peptides on papain activity, an inhibitory mechanism of group-2 phytocystatins and a regulatory mechanism of extended Ct peptide have each been proposed. By contrast, the antifungal activity of Nt peptide appeared to be greater than that of FL peptide, and the Ct peptide showed no effect on antifungal activity, indicating that the antifungal effect is not related to proteinase inhibitory activity. The results are valid for most phytocystatins with respect to the inhibitory mechanism against cysteine proteinase.

Phytocystatins are a class of reversibly binding cysteine proteinase inhibitors found in plants. These cysteine proteinase inhibitors lack disulfide bridges and possess a conserved N-terminal amino acid sequence [L-A-R-[FY]-A-[VI]-X(3)-N] [1]. Although the primary sequences of phytocystatins are more similar to the type II cystatins of animals, they are assigned to an independent family [1]. Phytocystatins have been reported to contain three motifs that are involved in the interaction with their target proteinases: (a) the active site motif QxVxG; (b) a G near N-terminus; and (c) a W in the second half of the protein [2,3]. However, according to molecular weight, they have been divided into three distinct groups. Most of the phytocystatins are included in group-1, such as oryzacystatin (OC)-I from rice, and

Abbreviations
BANA, N_a-benzoyl-D,L-arginine β-naphthylamide hydrochloride; Ct, C-terminus; FL, full-length; GST, glutathione *S*-transferase; Nt, N-terminus; OC, oryzacystatin.

they are usually 12–16 kDa in size and show high homology with chicken egg white cystatin [4]. The group-2 phytocystatins are approximately or greater than 23 kDa, such as those found in cabbage [5], soybean [6], taro [7], sesame [8] and strawberry [9]. They have a highly conserved N-terminal region, which is similar to that in group-1, and are tailed by a repetitive peptide at the C-terminus, in which variation is possibly caused by gene duplication [10]. The third group of phytocystatins, group-3, is found in potato [11] and tomato [12], and includes an 80 kDa multi-cystatin with eight cystatin domains. Phytocystatins show variable expression patterns during plant development and defense responses to biotic and abiotic stresses [13–15]. Although at least two functions have been assigned to phytocystatins, such as regulation of protein turnover and protection of plants against insects and pathogens [16], their physiological functions remain obscure.

The taro, *Colocasia esculenta*, is an important staple food of Taiwan aborigines, and is widely cultivated in local mountainous farms. This crop, especially Kaohsiung No. 1, is popular for its high productivity and lower susceptibility to pathogens. It might be expected that such taro corms display the characteristic mechanisms regulating protein turnover, as well as defense barriers towards pathogens. In a preliminary survey of proteinase inhibitors from taro tuber, copious amount of a cysteine proteinase inhibitor were discovered [7]. Recently, we isolated a group-2 phytocystatin from taro corms, named CeCPI, and demonstrated its anti-papain activity as well as anti-fungal activity [7]. In the alignment data, we also found that the group-2 phytocystatin is like a group-1 phytocystatin with the addition of a C-terminal extension. Moreover, the C-terminal region of the group-2 phytocystatin shares a high consensus sequence among the discovered species [7]. The C-terminal part is probably responsible for regulating inhibitory activity and target specificity. To obtain a better understanding of the structure and biochemical function of tarocystatin CeCPI, we amplified separately the intact full length (FL), N-terminal region (Nt) and C-terminal region (Ct) peptides by PCR and studied their relationship by in-gel anti-papain activity, inhibitory patterns and anti-fungal activity. Based on a comparative study of group-1 (Nt peptide) and group-2 (FL peptide), we discuss the inhibitory mechanism of group-2 phytocystatins and their evolutionary significance. In addition, both the inhibitory characteristics of the 'noncanonical' binding mode of group-2 phytocystatins towards papain and the 'canonical' binding mode of group-1 phytocystatins are addressed.

Results

Purification of recombinant proteins from *Escherichia coli* and in-gel inhibitory activity assay

The FL peptide comprises of 205 amino acids, including 98 amino acids of Nt peptide and 107 amino acids of Ct peptide. Expressed recombinant FL, Nt and Ct peptides were further purified from the *E. coli* and analyzed by 12.5% SDS/PAGE. Purified proteins of both FL and Nt peptides showed two bands, each with the lower band corresponding to a 27 kDa glutathione *S*-transferase (GST) protein, with the upper band corresponding to 56 kDa for GST-FL and 40 kDa for GST-Nt peptide fusion proteins (Fig. 1A). The Ct peptide showed only one band corresponding to 42 kDa (GST-Ct). The free recombinant proteins of the three peptides (Fig. 1B) were obtained by digesting off GST peptide and performing chromatography [1] for further biochemical analysis. The inhibitory activity of recombinant proteins was assessed by an in-gel activity assay and can be visualized by the clear zone of hydrolysis (Fig. 1C). By contrast, increasing the concentration of recombinant Ct peptide acting on papain confirmed that the Ct peptide enhanced its capacity (Fig. 1D).

Antifungal activity assay

A previous study showed that tarocystatin (i.e. FL peptide) has effective activity on hyphal growth inhibition against several phytopathogenic fungi [7]. In an attempt to compare the antifungal effect of different peptides of tarocystatin, a bioassay on mycelial growth of *Sclerotium rolfsii* was carried out. FL (group-2) and Nt (group-1) peptides exhibited apparent antifungal activity at a concentration > 3.4 nM, but no antifungal activity was observed in the Ct peptide bioassay (Fig. 2A). It appeared that Nt peptide (group-1) was more effective than the FL peptide (group-2) (Fig. 2B). Although antifungal activity of phytocystatins from taro, strawberry and chestnut has been reported previously [7,9,17], the mechanism of inhibitory activity of phytocystatins against phytopathogenic fungi remains unclear. The presence of the Ct peptide in the FL peptide appears to be the cause of the reduction in antifungal activity. The hyphal morphology was also observed under low and high magnification microscopy. The growth-retarded mycelium exhibited swelling, less branches and blunt tips at an Nt peptide concentration of 3.4 nM (Fig. 2C), and displayed swelling, no branches, very short tips and fragmentation at a concentration of 5.1 nM.

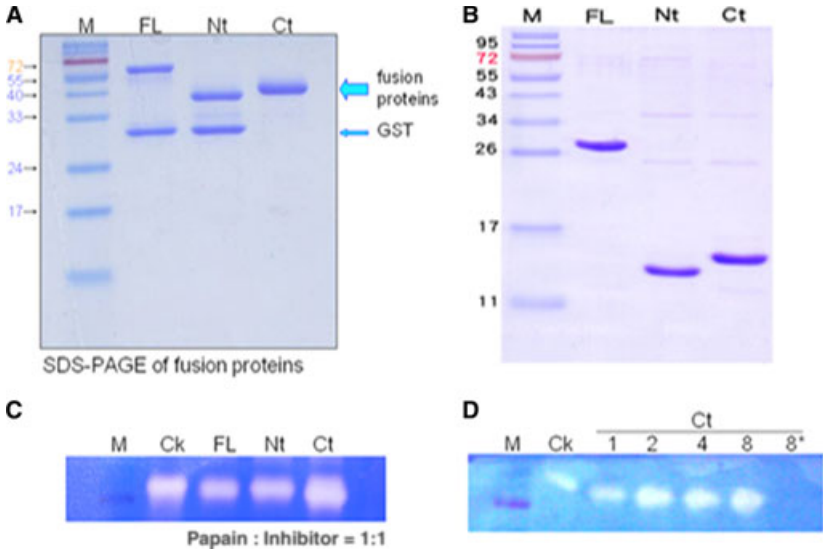

Fig. 1. Purification of recombinant proteins and their in-gel inhibitory activity assay. (A) SDS/PAGE analysis of purified recombinant GST-fused proteins from bacterial extracts. Lane M, protein standard; FL lane, two bands corresponding to GST-FL (upper band) and GST (lower band); Nt lane, GST-Nt peptide (upper band) and GST (lower band); Ct lane, only one band (GST-Ct peptide). (B) SDS/PAGE analysis of purified recombinant tarocystatin cleaved after thrombin digestion. (C) In-gel inhibitory activity assay for three different segment recombinant proteins. The band brightness is proportioned to papain activity Samples containing FL or Nt peptides reduce the brightness on the gel, indicating their inhibitory capacity. By contrast, the Ct peptide showed an enhancing capacity. (D) In-gel inhibitory activity assay for varied concentrations of the Ct peptide. The brightness of the band increased with increasing Ct peptide concentration, confirming its enhancing capacity. Lane 8* indicates a subject containing only Ct peptide recombinant protein, and not containing any papain, where no digestion occurred.

Inhibitory kinetics of different segments of tarocystatin on papain activity

Before inhibition analysis, the recombinant protein was purified by being passed through affinity columns and subsequently cleaved by thrombin and identified by SDS/PAGE analysis. Electrophoresis of free recombinant protein of FL, Nt and Ct peptides, showed maximum purity (Fig. 1B). To determine the inhibition constant, N_a-benzoyl-D,L-arginine β-naphthylamide hydrochloride (BANA) was used as a substrate at a concentration range of 20–260 μM for the assay with equimolar (25 nmol) papain and inhibitor concentrations (Fig. 3A). The Ct peptide curve appeared above the control (Ck), indicating that the Ct peptide enhances the enzyme activity, which is consistent with the anti-papain activity determined by the in-gel assay (Fig. 1C,D). Both FL and Nt peptides could inhibit papain activity by 55% and 39%, respectively, whereas Ct peptide activated papain by 18% (Table 1). Therefore, FL peptide exhibited mixed inhibition, Nt peptide exhibited competitive inhibition and Ct peptide exhibited allosteric activation (Fig. 3B).

Further verification of the inhibition characteristics was performed by repeating the experiment after making a slight modification, with BANA at a concentration in the range 60–240 μM, as well as varying the inhibitor level in the assay. A Lineweaver–Burk plot of the reactions with varied inhibitor levels again showed competitive inhibition for Nt peptide and mixed inhibition for FL peptide (Fig. 4A,B). Thus, the presence of two inhibition types was confirmed. The inhibition constants (K_i values) could be calculated from the apparent K_m and V_{max} changes (Table 1). The K_i value of Nt peptide (group-1) inhibition on papain was found to be 5.7×10^{-8} M. This value is very close to the K_i of rice OC-I (3.0×10^{-8} M) [18]. In addition, comparison of inhibitory activity with other group-1 species showed that K_i for Nt peptide of tarocystatin is lower than those for rice OC-II (8.3×10^{-7} M) [18], Job's tears cystatin (1.9×10^{-7} M) [19] and soybean cystatin L1 (1.9×10^{-5} M) [20], but higher than those for sesame (2.7×10^{-8} M) [8] and maize CCI (2.3×10^{-8} M) [21]. Nt peptide inhibitory activity appears to be intermediate among the group-1 phytocystatin family.

Hypothetical structural model of group-2 tarocystatin and the inhibitory mechanism

In mixed inhibition, the K_i value is separated into K_{ia} and K_{ib}. K_{ia} is described as the dissociation of inhibitor

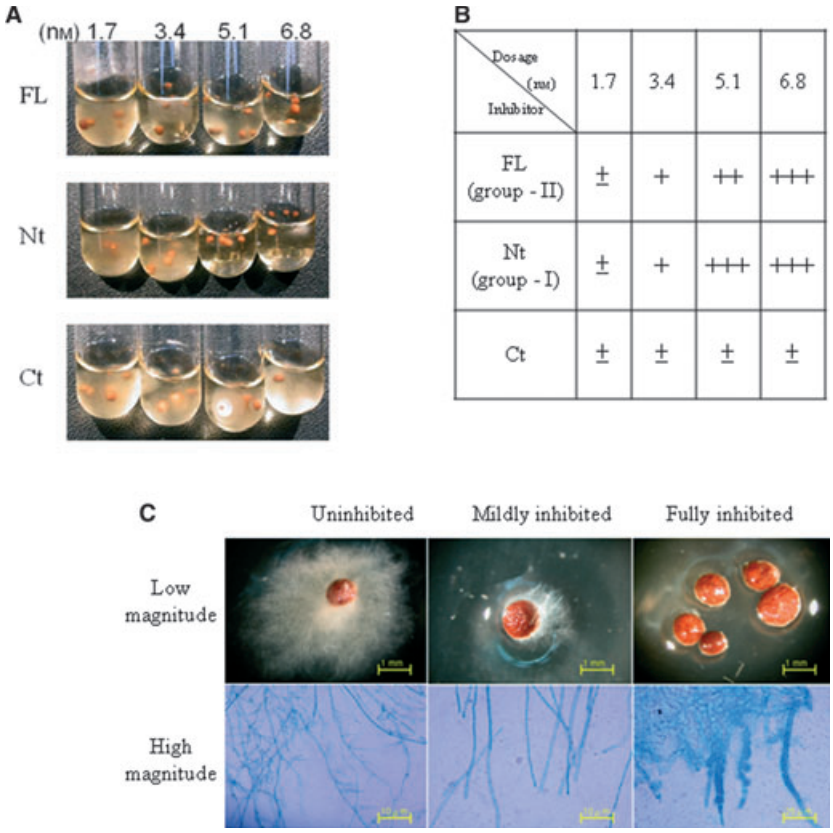

Fig. 2. Anti-fungal activity assay for recombinant proteins of different tarocystatin segments. (A) Five pieces of sclerotia cultured in the presence of recombinant proteins of varied concentrations in a 1-cm diameter glass tube. Inhibition efficacy is proportional to the clarity of the medium. Additional FL or Nt peptides in the sclerotia culture caused an increase in clarity of the medium, indicating their anti-fungal activity, whereas Ct peptide did not. (B) The inhibition level was graded from high effective (+++) to null (±) by visual quantification. (C) The different inhibitory strengths of varied FL peptide levels on mycelium growth was observed under high and low magnification. Mildly inhibited mycelium exhibited swelling, less branching and blunt tips. Fully inhibited mycelium exhibited more swelling, no branches, very short tips and fragmentation.

from enzyme, whereas K_{ib} is for that between the inhibitor and enzyme–substrate complex. A prominent characteristic of mixed inhibition compared to competitive inhibition is that the mixed inhibitors bind to enzymes as well as enzyme–substrate complexes, but competitive inhibitors bind only enzymes. Thus, the Ct peptide of tarocystatin may be able to dock onto the papain structure when the active site is occupied by a substrate. Furthermore, the occurrence of the K_{ib} value is always tailed with an unknown regulatory effect, indicating that the Ct peptide functions to alter the target protein conformation and prevent product formation. The Nt peptide functions like the entire OC-I and confers tarocystatin with an affinity for the competing active site.

The 3D structural model of tarocystatin was predicted to infer the interaction between group-2 tarocystatin and papain. The Ct peptide sequence shares 48% identity and 68% similarity with taro Nt (1–97 amino acids), as solved by NMR spectroscopy [22]. Although there was no established template for Ct peptide 3D structure prediction, it shares 13% identity and 38% similarity to group-1 OC-I (Fig. 5). Therefore, the Ct peptide structure was predicted using secondary structure estimation and a folding pattern simulation program with pseudo-energy minimization. Subsequently, the entire tarocystatin 3D structure was obtained by combining the structures of two segments. Its conformation resembled an earphone comprising two solid masses and a linear structure (Fig. 6). A highly structural similarity between the Nt and Ct peptides was found and, presumably, the Ct peptide compete with the Nt peptide for binding to the active site (Fig. 6). However, the assay using varied concentrations in the range 0–10 000 μM of Ct peptide to compete with the Nt peptide at a concentration of 62.5 μM did not demonstrate that the Ct peptide reduced the inhibitory capacity of the Nt peptide (Fig. 7A). Instead, it revealed that the Ct peptide does not act competitively.

To determine whether the connection between the Nt and Ct peptides is important for inhibitory capacity of the FL peptide, equal amounts of Nt and Ct peptides were mixed and the inhibitory capacity of the mixture was then compared with that of only the Nt or FL peptides. The curve of the mixture of Nt and Ct peptides did not tend to that of the FL peptide in the retrieve test (Fig. 7B). The pattern of competitive inhibition against papain by the Nt peptide of group-1 is consistent with the previous findings obtained for

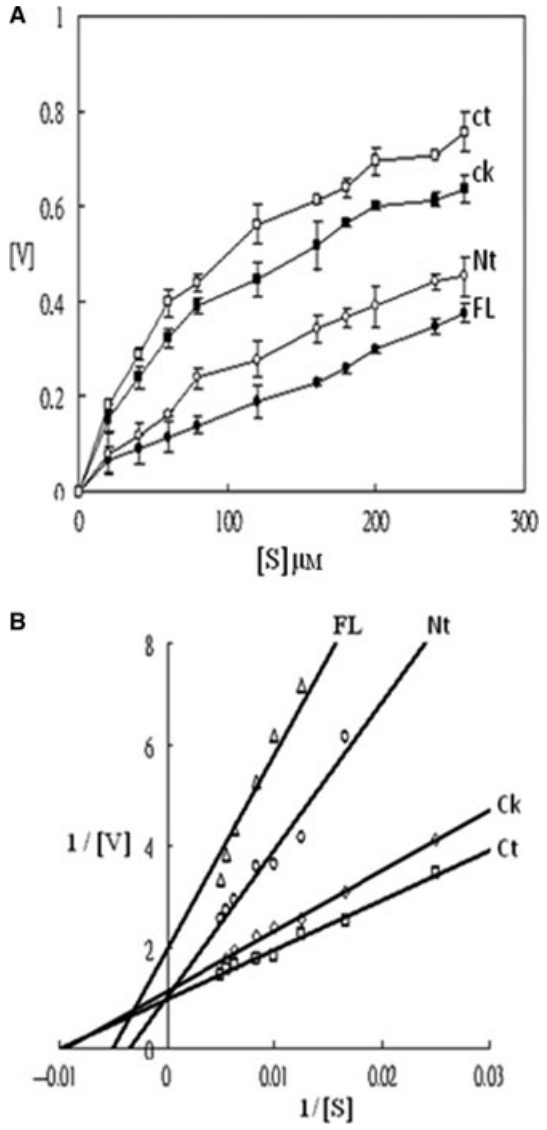

Fig. 3. Analysis of inhibitory kinetics of different tarocystatin segments. (A) Plot of papain activity for a single inhibitor concentration (0125 μM) at various substrate concentrations. ■, Ck (water instead of inhibitor); ●, FL peptide; ○, Nt peptide; □, Ct peptide. The *y*-axis is the catalytic velocity of papain, expressed as the change in optical density per unit time. The *x*-axis is the substrate concentration (mM). Each point represents the mean value of three repeated experiments, with the standard error shown as a bar. (B) Lineweaver–Burk plot for different tarocystatin segments, and also the double reciprocal plot of (A). Ck line crosses lines of the FL, Nt and Ct peptides in the second quadrant, *y*-axis and *x*-axis, respectively, indicating that the FL peptide behaves with mixed inhibition, the Nt peptide behaves with competitive inhibition and the Ct peptide behaves as an allosteric activator.

many other group-1 phytocystatins [18,19], whereas the mixed type inhibition against papain by FL peptides of group-2 has not been reported to date.

Table 1. Inhibitory characteristics and K_i values of diferent tarocystatin segments.

Model	Average (%) inhibitory activity	K_i value (μM)
FL peptide (group-2) mixed inhibition	55	K_{ia} 0.098, K_{ib} 0.252
Nt peptide (group-1) competitive inhibition	39	K_i 0.057
Ct peptide allosteric activation	−18	–

Information about mixed inhibition by other phytocystatins is scarce. A similar inhibition model, noncompetitive inhibition, was reported in strawberry FaCPI-1 [9] and in soybean L1 and R1 [20]. Of these, only FaCPI-1 belongs to the group-2 phytocystatins and demonstrates a strong inhibitory activity (1.9×10^{-9} M). The FaCPI-1 amino acid sequence is highly homologous with tarocystatin, but its mechanism cannot show mixed inhibition. To unravel the mechanism, a detailed investigation of the 3D structural interaction between group-2 phytocystatins and papain is necessary.

Discussion

In the present study we are the first to show the inhibition difference between group-1 and group-2 phytocystatins, and to examine the importance of the extended C-terminal region (Ct peptide of tarocystatin) with respect to interaction with anti-papain activity.

In the analysis of the primary structure of tarocystatin, we found that the group-2 tarocystatin (FL peptide) is a group-1 phytocystatin (Nt peptide) possessing an additional Ct peptide. Moreover, the Ct peptide of the group-2 phytocystatin shares a high consensus sequence among the discovered species [7]. Both the FL and Nt peptides exhibit a good inhibitory property on papain activity, whereas the Ct peptide exhibited papain activation that was also evident in an in-gel inhibitory assay (Fig. 1C). The inhibition constant demonstrated that the FL peptide exhibited mixed inhibition, and the Nt peptide exhibited competitive inhibition, suggesting a canonical binding mode as with many other group-1 phytocystatin species previously reported (Table 2). The enhancement of the proteinase activity by 18% (Table 1) implicates that the interaction between papain and the Ct peptide possesses refolding in the conformation change of the papain protein. The mixed type inhibition against papain by the FL peptide might be due to the presence

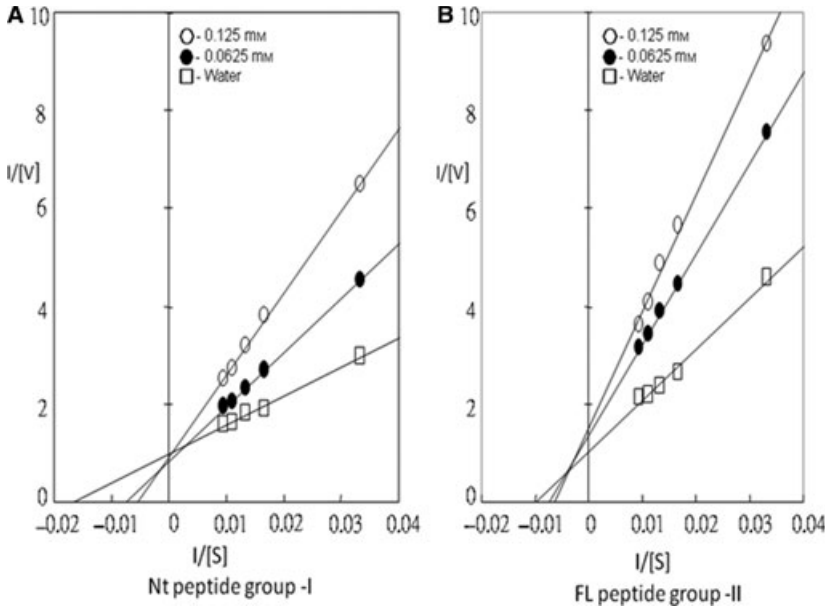

Fig. 4. Lineweaver–Burk plot for reactions in the presence of two different concentrations of Nt peptide (A) and FL peptide (B). The inhibitor concentrations were 0.125 mM (○) and 0.0625 mM (●) in each case. Water (□) was used as a control.

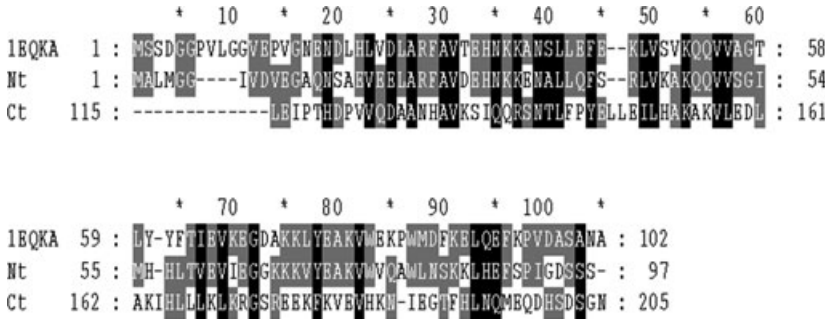

Fig. 5. Sequence alignment of the Nt and Ct peptides of taro and OC-I (Protein Data Bank: 1EQK). The identical residues are shown as a black box and the partially conserved residues are in grey. OC-I shares 48% identity and 68% positives with the Nt peptide of tarocystatin and 13% identity and 38% positives with the Ct peptide of tarocystatin.

of the Ct peptide, which plays an activation role on papain when used alone. Therefore, the mechanism of the Ct peptide with respect to enhancing papain activity presumably involves allosterically binding adjacent to the active/substrate binding site and altering the papain conformation to be more accessible for the substrate, which is defined as the 'noncanonical' binding mode, where these inhibitory characteristics are quite different from the 'canonical' binding mode of group-1 phytocystatins, as noted previously [23]. This change may also shift the orientation of the Nt peptide to bind with competitive inhibition and result in blocking the substrate from the approaching catalytic site. When the Ct peptide was bound to papain and linked with the Nt peptide, substrates still had the chance to bind to the active cleft. Nevertheless, the Nt peptide was so close to active cleft that allows Nt peptide binding prior to any approaching substrates. Thus, the enhancing effect of the Ct peptide was followed by an immediate binding of the Nt peptide. In this case, substrates still could reach the active cleft and be trapped by some inner pulling force, but could not be fixed in the catalytic site that the Nt peptide blocked. This mechanism was like a noncompetitive inhibition, where substrates could bind to the enzyme–inhibitor complex but not to be turned to products. However, if the Nt peptide bound to papain before the Ct peptide, tarocystatin would simply exhibit competitive inhibition. The alternative binding pattern strongly supports the idea that tarocystatin is a mixed type inhibitor, and provides evidence for the difference between group-1 and group-2 phytocystatins.

Phytocystatin has been known for its defense function against attack by insects and pathogens. These proteins have received much attention from researchers due to their potential utilization as bioinsectides in agrobiotechnology [3,4]. To extend our previous study on antifungal activity [7], a bioassay on mycelial growth of *S. rolfsii* was performed, and revealed that the FL and Nt peptides exhibited apparent antifungal

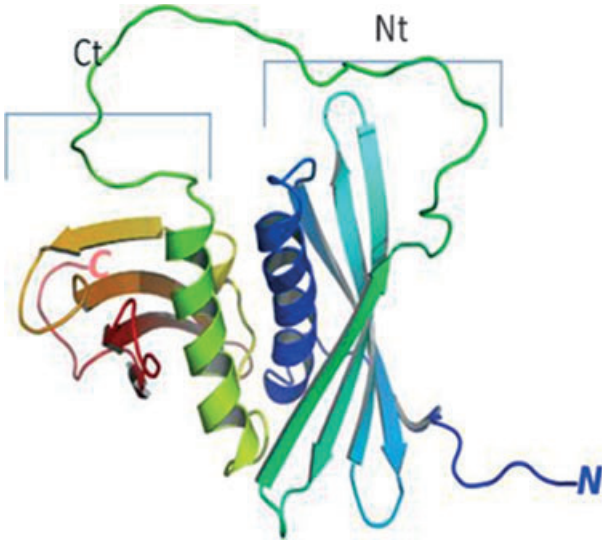

Fig. 6. Conjectural structure model of tarocystatin. Flat arrows and helical ribbons represent β-sheets and α-helix structures, respectively. The entire structure resembles an earphone comprising two solid masses and a linear structure.

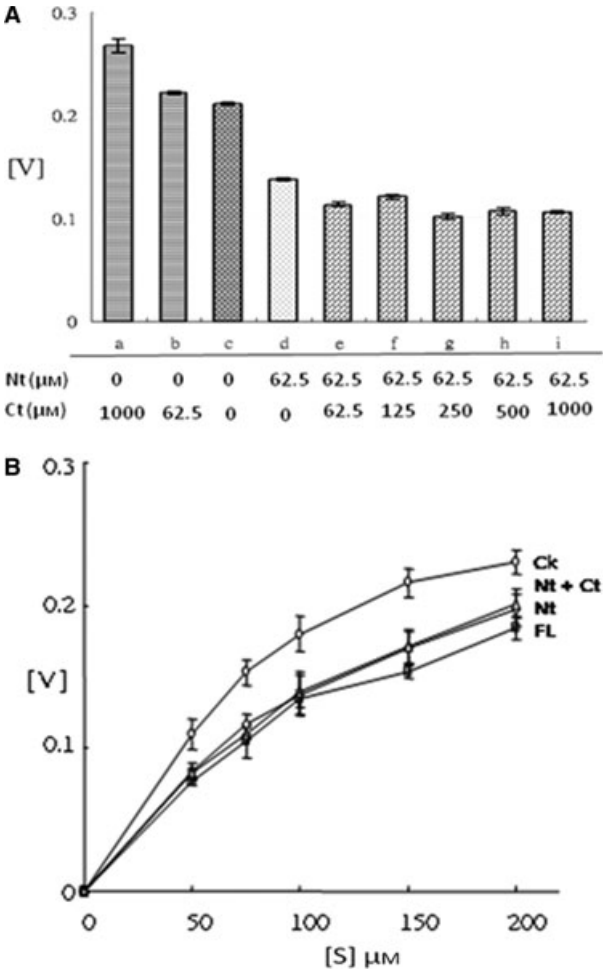

Fig. 7. Competition and retrieve test of the Ct peptide to Nt peptide. (A) Competition test: the *y*-axis is catalytic velocity of papain, which was measured as the change in optical density over time. Each reaction had the indicated amount of Ct and Nt peptides that reacted with papain. An increasing Ct level did not reduce the inhibitory capacity of the Nt peptide, but instead maintained a steady intensity. (B) Retrieve test: the mixture of Nt and Ct peptides of 625 μM was compared with an equal amount of only FL or Nt peptides in the reaction with varied substrate concentrations. The curve of Nt plus Ct peptides highly overlapped that of the Nt peptide, indicating that the Nt peptide cannot retrieve the inhibition efficacy of the FL peptide when it disconnects from the Ct peptide.

activity at a concentration above 3.4 nM, but no significant antifungal activity was observed for the Ct peptide (Fig. 2A,B). Microscopic observations indicated that the Nt peptide appeared to be stronger than FL peptide (Fig. 2B). Because the Ct peptide alone does not show any antifungal effect, this implies that the antifungal activity might be connected to the Nt peptide conformation. A reduction of antifungal activity *in vitro* by FL peptide may be due to a molecular mass difference. It has been speculated that the FL peptide is larger than the Nt peptide, making it more inefficient to diffuse inside hyphal cells. The true mechanism responsible for the antifungal activity of tarocystatin still requires further investigation.

To date, the physiological significance of the Ct peptide remains unknown. Accumulating evidence shows that this repeated domain may originate from gene duplication and be exploited for other functions [10]. Recent evidence also demonstrated that carboxy terminus-extended PhyCys have the capacity to inhibit human legumanin peptide due to the presence of the conserved motif SNSL and act as a bifunctional inhibitor [24]. Our findings focused on the Ct peptide on cysteine protease, which may function with three roles: (a) to endow the N-terminal domain with more specificity and inhibition to papain; (b) to prevent the N-terminal domain from rapid digestion by endogenous or exogenous peptidase; and (c) to enrich its molecular size as an ideal storage protein. Due to these beneficial characteristics, the Ct peptide could be reserved under evolutionary selection. Further studies, including mutagenesis and structural studies, are required to better understand the molecular mechanisms involved in the tarocystatin binding to papain and to identify the regulatory cleft involved in the inhibition process [15].

Based on the characterization of inhibitory function of group-1 and group-2 phytocystatins, we suggest that

Table 2. K_i values comparison among published group-1 phytocystatins. Both strawberry and soybean are noncompetitive type. The rest are competitive type.

Species	K_i value	Reference
Strawberry	1.9×10^{-9}	Martinez *et al.* [9]
Maize CCI	2.3×10^{-8}	Abe *et al.* [21]
Sesame	2.7×10^{-8}	Shyu *et al.* [8]
Oryza OC-I	3.0×10^{-8}	Kondo *et al.* [18]
Nt peptide (group-1 phytocystatin)	5.9×10^{-8}	Present study
Soybean	1.9×10^{-7}	Misaka *et al.* [6]
Job's tear	1.9×10^{-7}	Yaza *et al.* [19]
nTaMDC 1	5.8×10^{-7}	Christova *et al.* [32]
Oryza OC-II	8.3×10^{-7}	Kondo *et al.* [18]
WC5	10^{-6}	Corre-Menguy *et al.* [33]

group-1 and group-2 both evolved from a common ancestor. The evolutionary direction from group-1 toward group-2 by gene duplication appears to be an adaptation resulting from an evolutionary 'arms race' of rapid change in both interacting proteins.

Experimental procedures

Construction of three DNA regions of the *CeCPI* gene

Three different segments of the *CeCPI* gene were amplified by PCR (Pfu; Stratagene, La Jolla, CA, USA). These DNA segments correspond to the coding regions of the FL, Nt and Ct peptides. Two forward (F1 and F2) and two reverse (R1 and R2) primers were designed to amplify the genes: F1, 5′-TTGGATCCATGGCCTTGATGGGGGC-3′; R1, 5′-TTGAATTCTTTCCAGAGTCTGAATGATC-3′; F2, 5′-TTGGATCCTCGGTTACGCCAGCAGAT-3′; R1, 5′-TTGAATTCTTTCCAGAGTCTGAATGATC-3′; F2, 5′-TTGGATCCTCGGTTACGCCAGCAGAT-3′; and R2, 5′-TTGAATTCGAATCGCCAATGGGGCT -3′.

The underlined bases in the primers indicate restriction sites for *Bam*HI (GGATCC) or *Eco*RI (GAATTC). The primer combination of F1 and R1 was used for amplification of the FL peptide; F1 and R2 was for the Nt peptide, and F2 and R1 was for the Ct peptide. The PCR products were digested with *Bam*HI and *Eco*RI, and ligated to pGEX-2TK vector (Amersham Biosciences, Piscataway, NJ, USA) at the corresponding restriction sites.

Expression, purification and characterization of recombinant tarocystatin

E. coli BL21 (DE3) cells containing the appropriate construct were grown at 37 °C in 2YTA liquid medium until D_{600} of 1.5 was reached. The recombinant CeCPI expression was induced by addition of 1 mM isopropyl-β-D-thiogalactopyranoside. Two hours after induction, the recombinant proteins were extracted from 250 mL of bacterial culture by using B-PER® GST-fusion protein purification kit (Pierce No. 78400; Pierce Biotechnology, Rockford, IL, USA). For the assay of inhibitory kinetics of CeCPI fragments, the GST fusion protein was cleaved with 20 units of thrombin for 16 h at room temperature. Finally, the recombinant proteins were collected by passing the extract through a glutathione Sepharose 4B affinity column (Amersham Biosciences). The protein was quantitated with a Bio-Rad protein assay kit (Bio-Rad, Hercules, CA, USA) using BSA as a standard.

In-gel antipapain assay

Qualitative analysis of CeCPI protein was performed according to Michaud *et al.* [25] on 12.5% SDS/PAGE containing 1% gelatin. A mixture of CeCPI proteins and papain was first incubated at 37 °C for 15 min in a mildly denaturing buffer (62.5 mM Tris–HCl, pH 6.8; 2% SDS, 2% sucrose; 0.01% bromophenol blue), and then subjected to electrophoresis using a Hoefer SE250 system (Hoefer, Inc., Holliston, MA, USA). After migration, the gels were transferred to a 2.5% v/v aqueous solution of Triton X-100 for 30 min at room temperature to allow renaturation followed by incubating in reactive buffer (100 mM sodium phosphate, pH 6.8, containing 8 mM EDTA, 10 mM L-cysteine and 0.2% Triton X-100) for 75 min at 37 °C. Subsequently, the gels were rinsed with water and stained with Coomassie Brilliant Blue. Proteinase inhibitor activity was visualized as clear zones on a blue background and the intensity of the clear band is inversely related to the inhibition level.

Inhibitory tests and determination of K_i values

K_i values of papain inhibition were determined from Lineweaver–Burk plots, a double reciprocal plot of substrate concentration versus velocity. The velocity was determined by measuring the A_{540} of the chromophore, as described by Pernas *et al.* [17]. Briefly, an appropriate amount of inhibitor was pre-incubated with 1 μM of papain in 100 μL of reaction mixture containing 0.1 M sodium phosphate buffer (pH 6.5), 10 mM EDTA and 10 mM 2-mercaptoethanol at 37 °C for 10 min. The reaction was started by the addition of 100 μL of a varied concentration in the range 20–260 μM of BANA (Sigma, St Louis, MO, USA) as substrate. The reaction mixture was incubated at room temperature for 20 min and 300 μL of 2% HCl in ethanol (w/v) was added to stop the reaction. The chromophore was then developed by addition of 300 μL of 0.06% *p*-dimethylaminocinnamaldehyde in ethanol followed by incubation at room temperature for 15 min and measurement of A_{540}.

The inhibitory activity was recorded as the inhibition percentage (%) and the inhibition percentage (I%) of papain was calculated using the equation:

$$I\% = \frac{T - T^*}{\mathrm{T}} \times 100$$

where, T and T* are the velocities in the absence and presence of the inhibitor from reactions, respectively. The average inhibitory activity was calculated from I% values of varied substrate concentrations.

Antifungal activity assay of different regions of tarocystatin

The fungal activity assay was performed as described previously [7]. Five pieces of sclerotia of phytopathogenic fungus *S. rolfsii* were cultured in 1 mL of half strength potato dextrose broth, which contained purified GST-tarocystatin segment fusion proteins at concentrations of 1.7, 3.4, 5.1 and 6.8 nM in four separate sets. The fungi were cultured at 28 °C under continuous shaking (200 r.p.m.) on an orbital shaker for 72 h. Hyphal growth inhibition by tarocystatin segment proteins was observed directly, as well as under a microscope.

Conjectural tarocystatin 3D structure simulation

The tarocystatin primary sequence (AAM88397) was subjected to NCBI psi-BLAST with a threshold of 0.0001 for searching for homologous sequences from various plants. The sequence similarities of 18 amino acid sequences were distributed with the highest identities of 66% and a positive of 83% for soybean to the lowest identities of 55% and a positive of 77% for tomato, excluding nonplant and multidomain cystatin homologs. These 18 sequences were aligned using CLUSTALW [26] and shaded with GENEDOC [27] software. The secondary structure of these 18 sequences was analyzed by two programs, PSI-PRED [28] and YASPIN [29]. The results obtained by the two programs were consistent with each other and showed that both Nt and Ct peptide secondary structures were arranged in a similar pattern. This was also verified by aligning the OC-I with the tarocystatin Nt and Ct peptide regions. Therefore, the stereofolding pattern of OC-I [22] can be taken as a template for the CeCPI folding prediction by MODELER 8.1 [30]. The two structural conformations were merged after analysis by the automatic docking system, ZDOCK 2.3 [31], and then remodeled by MODELER 8.1 [30].

Acknowledgements

The present study was supported by the National Science Council, Taiwan, under project NSC-95-2317-B-002-005 to Kai-Wun Yeh. We thank Dr Michael Conrad (University of North Carolina at Chapel Hill) for critically reading the manuscript and for his helpful suggestions.

References

1 Margis R, Reis EM & Villeret V (1998) Structural and phylogenetic relationships among plant and animal cystatins. *Arch Biochem Biophys* **359**, 24–30.
2 Machleidt W, Thiele M, Laber B, Assfalg-Machleid I, Esterl A, Wiegand G, Kos J, Turk V & Bode W (1989) Mechanism of inhibition of papain by chicken egg white cystatin. *FEBS Lett* **243**, 234–238.
3 Arai S, Watanabe H, Kondo H, Emori Y & Abe K (1991) Papain-inhibitory activity of oryzacystatin, a rice seed cysteine proteinase inhibitor, depends on the central Gln-Val-Val-Ala-Gly region conserved among cystatin superfamily members. *J Biochem (Tokyo)* **109**, 294–298.
4 Abe K, Emori Y, Kondo H, Suzuki K & Arai S (1987) Molecular cloning of a cysteine proteinase inhibitor of rice (oryzacystatin). Homology with animal cystatins and transient expression in the ripening process of rice seeds. *J Biol Chem* **262**, 16793–16797.
5 Lim CO, Lee SI, Chung WS, Park SH, Hwang I & Cho MJ (1996) Characterization of a cDNA encoding a cysteine proteinase inhibitor from chinese cabbage (*Brassica campestris* L. ssp. pekinensis) flower buds. *Plant Mol Biol* **30**, 373–379.
6 Misaka T, Kuroda M, Iwabuchi K, Abe K & Arai S (1996) Soyacystatin, a novel cysteine proteinase inhibitor in soybean, is distinct in protein structure and gene organization from other cystatins of animal and plant origin. *Eur J Biochem* **240**, 609–614.
7 Yang AH & Yeh KW (2005) Molecular cloning, recombinant gene expression, and antifungal activity of cystatin from taro (*Colocasia esculenta* cv. Kaohsiung No.1). *Planta* **221**, 493–501.
8 Shyu DJH, Chou WM, Yiu TJ, Lin CPC & Tzen JTC (2004) Cloning, functional expression, and characterization of cystatin in sesame seed. *J Agric Food Chem* **52**, 1350–1356.
9 Martinez M, Abraham Z, Gambardella M, Echaide M, Carbonero P & Diaz I (2005) The strawberry gene Cyf1 encodes a phytocystatin with antifungal properties. *J Exp Bot* **56**, 1821–1829.
10 Christeller JT (2005) Evolutionary mechanism acting on proteinase inhibitor variability. *FEBS J*, **272**, 5710–5722.
11 Waldron C, Wegrich LM, Merlo PAO & Walsh TA (1993) Characterization of a genomic sequence coding for potato multicystatin, an eight-domain cysteine proteinase inhibitor. *Plant Mol Biol* **23**, 801–812.
12 Wu J & Haard NF (2000) Purification and characterization of a cystatin form the leaves of methyl

jasmonate-treated tomato plants. *Comp Biochem Physiol C Toxicol Pharmacol* **127**, 209–220.
13 Felton GW & Korth KL (2000) Trade-offs between pathogen and herbivore resistance. *Curr Opin Plant Biol* **3**, 309–314.
14 Botella MA, Xu Y, Prabbha TN, Zhao Y, Narasimhan ML, Wilson KA, Nielsen SS, Bressan RA & Hasegawa PM (1996) Differential expression of soybean cysteine proteinase inhibitor genes during development and in response to wounding and jasmonate. *Plant Physiol* **112**, 1201–1210.
15 Solomon M, Belenghi B, Delledonne M, Menachem E & Levine A (1999) The involvement of cysteine proteases and protease inhibitor genes in the regulation of programmed cell death in plants. *Plant Cell* **11**, 431–443.
16 Turk V & Bode W (1991) The cystatins: protein inhibitors of cysteine proteinase. *FEBS Lett* **285**, 213–219.
17 Pernas M, Sánchez-Monge R, Gómez L & Salcedo G (1998) A chestnut seed cystatin differentially effective against cysteine proteinases from closely related pests. *Plant Mol Biol* **38**, 1235–1242.
18 Kondo H, Abe K, Nishimura I, Watanabe H, Emori Y & Arai S (1990) Two distinct cystatin species in rice seeds with different specificities against cysteine proteinases. *J Biol Chem* **265**, 15832–15837.
19 Yoza K, Nakamura S, Yaguchi M, Haraguchi K & Ohtsubo K (2002) Molecular cloning and functional expression of cDNA encoding a cysteine proteinase inhibitor, cystatin, from Job's tears (*Coix lacryma-jobi* L. var Ma-yuen Stapf). *Biosci Biotechnol Biochem* **66**, 2287–2291.
20 Zhao Y, Botella MA, Subramanian L, Niu X, Nielsen SS, Bressan RA & Hasegawa PM (1996) Two wound-inducible soybean cysteine proteinases have greater insect digestive proteinase inhibitory activities than a constitutive homolog. *Plant Physiol* **111**, 1299–1306.
21 Abe M, Abe K, Iwabuchi K, Domoto C & Arai S (1994) Corn cystatin I expressed in *Escherichia coli*: investigation of its inhibitory profile and occurrence in corn kernels. *J Biochem (Tokyo)* **116**, 488–492.
22 Nagara N, Kudo K, Abe S, Arai M & Tanokura X (2000) Three dimensional solution structure of oryza cystatin-I, a cysteine proteinase of the rice, *Oryza sativa* L japonica. *Biochemistry* **39**, 14753–14760.
23 Bode W & Huber R (2000) Structural basis of the endoproteinase-protein inhibitor interaction. *Biochim Biophys Acta* **1477**, 241–252.
24 Martinez M, Diaz-Mendoza M, Carrillo L & Diaz I (2007) Carboxy terminal extended phytocystation are bifunctional inhibitors of papain and legumanin cysteines proteinases. *FEBS Lett* **581**, 2914–2918.
25 Michaud D, Cantin L, Raworth DA & Vrain TC (1996) Assessing the stability of cystatin/cysteine proteinase complexes using mildly-denaturing gelatin polyacrylamide gel electrophoresis. *Electrophoresis* **17**, 14–19.
26 Thompson JD, Higgins DG & Gibson TJ (1994) CLUSTAL W: improving the sensitivity of progressive multiple sequence alignment through sequence weighting, position-specific gap penalties and weight matrix choice. *Nucleic Acids Res* **11**, 4673–4680.
27 Nicholas KB, Nicholas HB Jr & Deerfield DW II (1997) GeneDoc: analysis and visualization of genetic variation. *EMBNEW News* **4**, 14.
28 McGuffin LJ, Bryson K & Jones DT (2000) The PSIPRED protein structure prediction server. *Bioinformatics* **16**, 404–405.
29 Lin K, Simossis VA, Taylor WR & Heringa J (2005) A simple and fast secondary structure prediction algorithm using hidden neural networks. *Bioinformatics* **21**, 152–159.
30 Sali A & Blundell TL (1993) Comparative protein modelling by satisfaction of spatial restraints. *J Mol Biol* **234**, 779–815.
31 Chen R, Li L & Weng Z (2003) ZDOCK: an initial-stage protein-docking algorithm. *Proteins* **52**, 80–87.
32 Christova PK, Christov NK & Imai R (2006) A cold inducible multidomain cystatin from winter wheat inhibits growth of the snow mold fungus, *Microdochium nivale*. *Planta* **223**, 1207–1218.
33 Corr-Menguy F, Cejudo FJ, Mazubert C, Vidal J, Lelandais-Brière C, Torres G, Rode A & Hartmann C (2002) Characterization of the expression of a wheat cystatin gene during caryopsis development. *Plant Mol Biol* **50**, 687–698.